

Development of a 3.8 meter variable polarization undulator (EPU)

Alex Deyhim, Aaron Lyndaker, Dave Waterman, Dave Caletka, Michael Rowen*,
Thomas Rabedeau*, K. Ingvar Blomqvist**

Advanced Design Consulting USA, 126 Ridge Road, P.O. Box 187, Lansing, NY 14882, USA

** Stanford Linear Accelerator Center, 2575 Sand Hill Road, Menlo Park, CA 94025*

***Consultant*

Abstract. The design of a Variable Polarization Undulator (EPU) of the four row, pure permanent magnet undulator and a length of 3.8 m is presented. The design requirements and mechanical difficulties for holding, positioning, and driving the magnetic arrays are explored. The structural and magnetic considerations that influenced the design are then analyzed. This undulator will be installed on a new beam line for materials science research, designated BL13 at Stanford Synchrotron Radiation Laboratory (SSRL) BL13 is being designed for the photon energy range from 250 to 1600 eV, and to utilize an undulator source that produces linear polarized radiation at variable azimuthal angles as well as both left and right circularly and elliptically polarized radiation.

Keywords: Insertion Devices, Magnets, Variable Polarization Undulator (EPU)

PACS: 07.07.-a, 07.85.Qe, 07.55.Ge.

INTRODUCTION

Advanced Design Consulting USA, Inc. (ADC), in collaboration with the Stanford Linear Accelerator Center (SLAC), has designed a 3.8m PPM EPU that will be delivered March, 2007. Particular attention has been paid to the magnetic design and structural integrity of the undulator.

MAGNETIC DESIGN

The magnets used in the ID must survive a specified exposure of 10^8 rads of ionizing radiation per year for ten years with no degradation. $\text{Sm}_2\text{Co}_{17}$ was therefore chosen for the magnet material. A minimum remanance of 1.05 T, was assumed for the magnetic design.

The undulator specifications require a minimum energy of 250 eV in elliptical mode. Phase error is limited to 5° in all polarizations. These requirements were met with a period of 56.9mm using 40 x 40mm blocks at a gap of 13.5mm. 129 full-strength poles have been used which, with end-sections gives a length of approximately 3.716m.

The effective fields, k-values and photon energies are given in Table 1 for the planar horizontal, planar vertical, circular and the polarization plane inclined 45° . The much higher photon energy for the 45° phase compared to the circular phase is due to a longitudinal field component present in the inclined mode of operation but absent in the elliptical polarization mode. The longitudinal component reduces the transverse field component and reduces the effective k-value.

Radia [1] was used to investigate the properties of the EPU. A model undulator with 17 poles was used for the evaluation. In the elliptical mode of operation the vertical field is symmetric, the horizontal field asymmetric. In the inclined plane mode of operation both the horizontal and vertical fields are symmetric.

The limits on the field integrals, integrated multipoles, transverse roll off and their derivatives are summarized in Table 2.

A model undulator with 17 poles was used to optimize the magnetic design. shows the vertical first integral as functions of x for planar, circular, vertical and 45° inclined plane

Phase	Effective Horiz. Flux Density (T)	Effective Vert. Flux Density (T)	k-value	Photon Energy (eV)
Planar	-	0.8053	4.27	148.7
Circular	0.4814	0.4814	2.55	200.0
Vertical	0.6029	-	3.20	245.5
45°	0.3435	0.3435	1.82	348.3

Table 1: Effective fields, k-values and photon energies.

The Ninth International Conference on Synchrotron Radiation Instrumentation
 May 28 – June 2, 2006, DAEGU, EXCO, KOREA

Parameter (All positions in cm)	Value
1 st horiz. Field Integral, $ X \leq 2.5, Y=0$	$ \int B_x dz \leq (40+75 X)$ G-cm
1 st vert. Field Integral, $ X \leq 2.5, Y=0$	$ \int B_y dz \leq (100+50 X)$ G-cm
Derivative of 1 st integral, $ X \leq 2.5, Y=0$	$ \partial(\int B_{x,y} dz) / \partial x \leq (50+150 X)$ G
2 nd horiz. Field Integral, $ X \leq 2.5, Y=0$	$ \int \int B_x dz dz' \leq (5000+10000 X)$ G-cm ²
2 nd vert. Field Integral, $ X \leq 2.5, Y=0$	$ \int \int B_y dz dz' \leq (15000+10000 X)$ G-cm ²
Integrated quadrupole field, $X = Y = 0$	≤ 50.0 G
Integrated sextupole field, $X = Y = 0$	≤ 75.0 G/cm
Integrated octupole field, $X = Y = 0$	≤ 40.0 G/cm ²
Peak field roll off 1 st derivative, $ X \leq 2.5, Y=0$	$ \partial B_y / \partial x \leq (870+440 X)$ G/cm
Peak field roll off 2 nd derivative, $ X \leq 2.5, Y=0$	$ \partial^2 B_y / \partial x^2 \leq (1200+1500 X)$ G/cm ²

Table 2: Limits on field integrals, multipoles, transverse roll-off and their derivatives.

mode of operation at 13.5 mm gap. All integrals are well within the specified limits.

Figure 2 shows the vertical first integrals as a function of x for planar, circular, vertical and 45° inclined plane modes at minimum gap. Of the horizontal first integrals only the 45° mode is non-zero due to the undulator's symmetry. All integrals are well within the specified limits.

Figure 3 shows the on-axis integrals at minimum gap as functions of the undulator phase for the inclined plane mode of operation. In contrast to the elliptical mode, both the horizontal and vertical first integrals are non-zero. The horizontal integral is small, but the vertical integral grows at large values of the undulator phase. It is, however, well within the specified values limits.

The second integrals of the full-size undulator can be extrapolated from the model. The result is shown in Table 3. All values are within the specified range, except for the second integral of B_x for the vertical mode. However, it can easily be reduced by using a long correction coil with horizontal field.

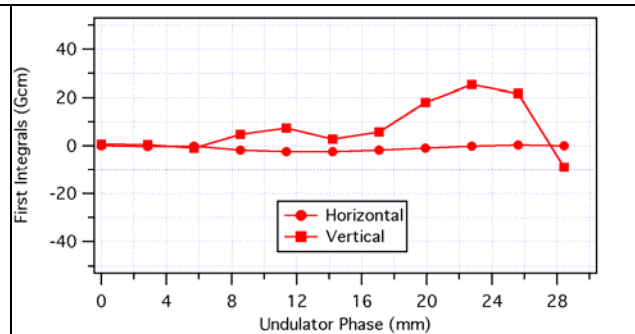
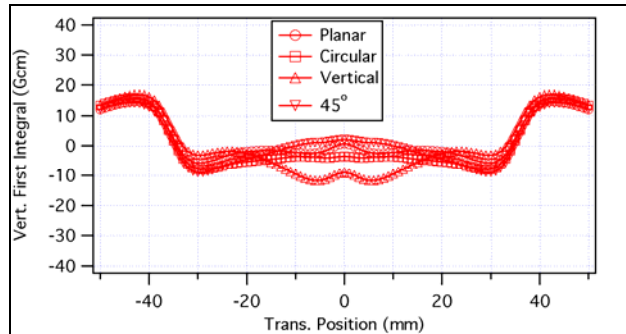


Figure 2: The vertical first integrals as function of x for planar, circular, vertical and 45° phases at minimum gap. Figure 3: The first integrals at minimum gap for the inclined plane mode as functions of the undulator phase.

Orbits calculated for circular and 45° inclined modes are shown in Figure 1. In circular mode the orbit is offset about 0.5 μm in both x and y inside the undulator. The 0.5 μm horizontal offset is also present in the inclined mode but there is no vertical offset.

Mode	$\int \int B_x dz dz'$ (Gcm ²)	$\int \int B_y dz dz'$ (Gcm ²)
Planar	0	2230
Circular	-3070	3340
Vertical	-6310	2910
45°	-530	2550

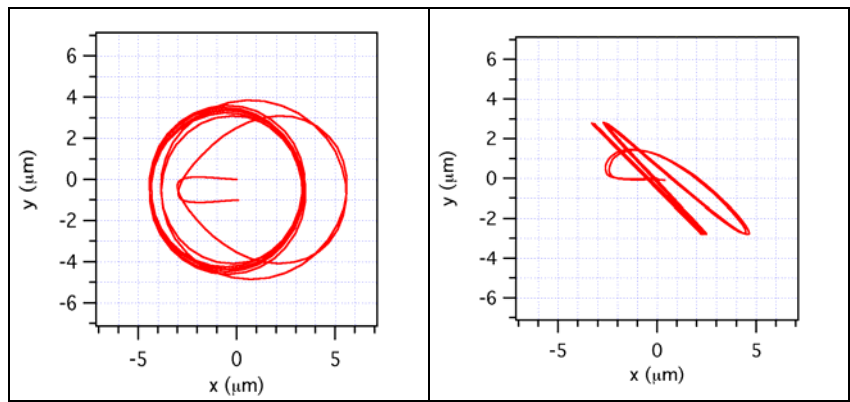


Table 3: The second integrals extrapolated for the full size undulator. Figure 1: Electron orbits projected on the (x,y) plane for the circular mode (left) and 45° inclined mode.

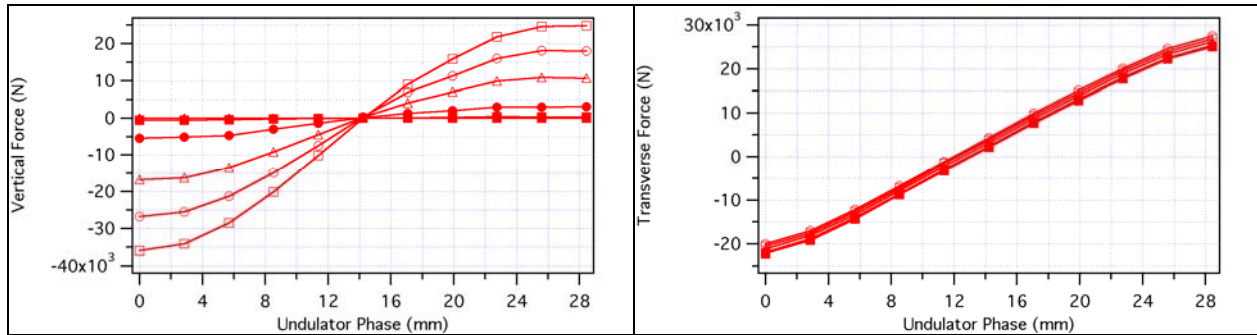


Figure 4: The vertical (left) and transverse (right) forces acting on the top girder in inclined plane mode.

Magnetic forces acting on the magnet girders have been calculated for each mode. Transverse forces act to rotate adjacent magnet arrays about the longitudinal axis while vertical forces cause girder deflections. Longitudinal forces determine the sizing of the motors. Each changes with phase and gap.

Figure 4 shows the vertical force applied to the upper girder at gaps of 13.5 to 100 mm as a function of undulator phase. At minimum gap the forces are very large and the girder must be extremely rigid if significant phase errors are not to be introduced. The effect of transverse forces, shown in the right hand portion of the figure, is minimized by bearing design.

The results of these analyses were input to a detailed finite element model of the undulator structure. A similar analysis of the forces acting on individual magnets was used to model the magnet holders. Both are described below.

STRUCTURAL ANALYSIS

A goal of the mechanical design was to limit the effect of deflections and rotations of the magnet arrays so that their contribution to the rms phase error was less than 0.5° in all operating modes. A total of eleven design iterations have so far been undertaken in order to meet this goal. Deflections of the strong-back, the bearings, the magnet girders, the magnet holders and the drive hardware have all evaluated.

As an example the effect of design changes on the deformation of the ID in horizontal mode is shown in Figure 5. In this mode the vertical force can be as high as 36 kN at minimum gap. Strong-back design, material changes, bearing selection, lead-screw diameter, and ball-nut mounts have all been considered. Design optimization reduced the deformations to $2.2 \mu\text{m}$ and the resulting rms phase error to 0.32° .

Deformations within the phase drive when operating in inclined plane mode are shown in Figure 6. Contours show the longitudinal deformation. Although the deflection is relatively large it can be removed by the control system. Absolute encoders are used on the longitudinal sub-girders for this reason.

A seismic analysis has also been undertaken. Modal analysis was used to determine loads acting on the support feet and at the anchor plates and tension rods under $0.65g$ ground acceleration in horizontal and vertical directions.

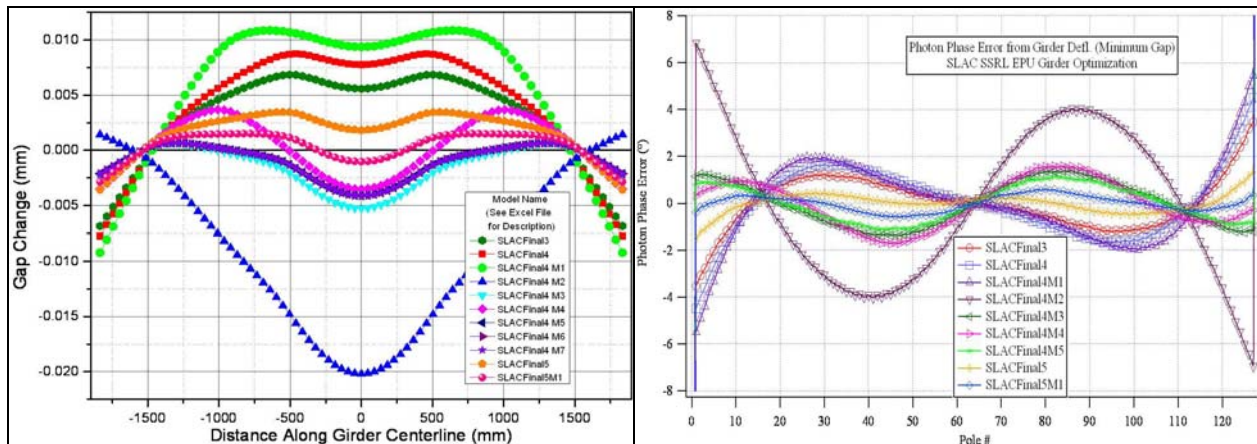


Figure 5: Vertical deformation of the magnet array (left) and the resulting phase error (right) in horizontal mode.

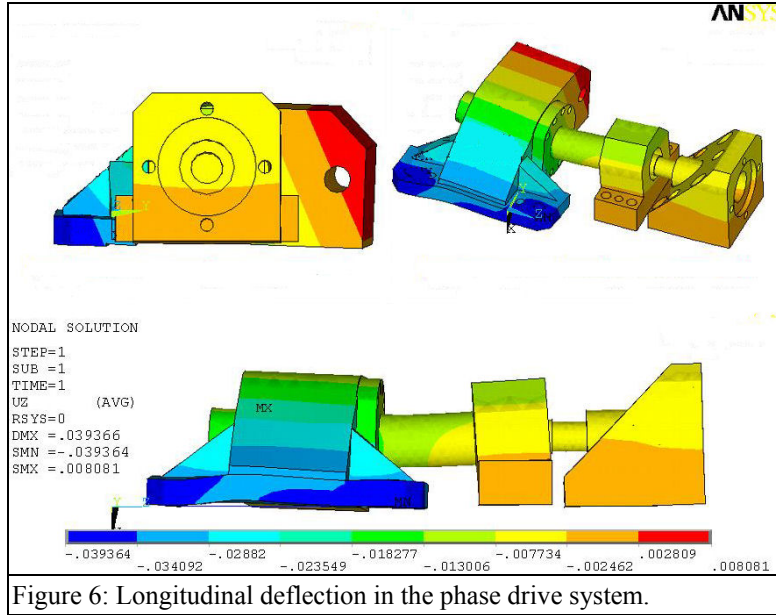


Figure 6: Longitudinal deflection in the phase drive system.

Tension links and contact surfaces were used in the finite element model to generate loads for input to Hilti PROFIS 1.6.11 software. The analysis showed that the geometry is adequate for all 3/4" HVA anchor styles using a 10" depth.

Magnet shimming is to be done using a screw-driven wedge and slide mechanism. While this simplifies the task of magnet shimming it introduces additional compliance into the system. The range of forces acting on individual magnets is about 160N in the y- and z-directions and 260N in x.

Surface-contact elements were used in the model, along with pre-tensioned members to simulate the bolts. Friction between adjacent magnets was neglected. Magnetic forces were applied as surface pressures. Analysis results are given in Table 4.

Vertical and transverse deflections are extremely small, however, those in the longitudinal direction can be as much as 70 μm. The effect on phase error should not, however, be severe – deflection of all magnets in the array will result in a change in the inclination angle in inclined plane or helical modes that can be compensated using the look-up table that relates undulator phase to polarization angle.

Load Direction	V-Blocks				H-Blocks			
	Force (N)	δ (μ)			Force (N)	δ (μ)		
		X	Y	Z		X	Y	Z
Transverse (X)	-50 to 40	2.12	0.87	0	-160 to 100	6.12	2.52	0
Longitudinal (Z)	-75 to 50	0	0	54.9	-160 to 0	0	0	70.3
Vertical (Y)	-360 to -200	1.57	2.16	0	225 to 300	0.74	1.01	0

Table 4: The range of loads and deflections acting on the magnets and their holders.

CONCLUSIONS

The final design review for this machine has been completed and parts are currently being manufactured at ADC.

ACKNOWLEDGMENTS

Portions of this research were carried out at the Stanford Synchrotron Radiation Laboratory, a national user facility operated by Stanford University on behalf of the U.S. Department of Energy, Office of Basic Energy Sciences.

REFERENCES

- [1] Radia was written at the ESRF by Pascal Elleaume and Oleg Chubar and can be obtained from <http://www.esrf.fr>